

# Conformational Stability of Human Interferon-Gamma on Association with and Dissociation from Liposomes

M. L. VAN SLOOTEN,<sup>1</sup> A. J. W. G. VISSER,<sup>2</sup> A. VAN HOEK,<sup>2</sup> G. STORM,<sup>1</sup> D. J. A. CROMMELIN,<sup>1</sup> W. JISKOOT<sup>1</sup>

<sup>1</sup> Department of Pharmaceutics, Utrecht Institute for Pharmaceutical Sciences (UIPS), Faculty of Pharmacy, Utrecht University, P.O. Box 80.082, 3508 TB Utrecht, The Netherlands

<sup>2</sup> MicroSpectroscopy Centre, Department of Biomolecular Sciences, Wageningen University, Wageningen, The Netherlands

Received 7 March 2000; revised 5 June 2000; accepted 22 August 2000

**ABSTRACT:** The integrity of a therapeutic protein has to be safeguarded when formulated in delivery systems such as liposomes. In this study, we investigated the conformational stability of recombinant human interferon gamma (hIFN $\gamma$ ) on association with and after dissociation from liposomal bilayers using circular dichroism (CD) and steady-state fluorescence spectroscopy as well as time-resolved fluorescence methodology. We used hIFN $\gamma$  adsorption to and desorption from empty liposomes as a model for hIFN $\gamma$ -containing liposomes prepared via the film hydration method. CD studies indicated that no changes in the secondary and tertiary protein structure occur during and after interaction of hIFN $\gamma$  with the liposomes. Steady-state fluorescence emission spectra of untreated and liposome-desorbed hIFN $\gamma$  revealed that the environment of the sole Trp residue was not affected by the adsorption/desorption process. The Trp-36 residue remained fully quenchable by acrylamide after desorption of hIFN $\gamma$  from the liposomes. Time-resolved fluorescence studies were conducted to probe the local environment and the mobility of Trp-36 before, during, and after interaction of hIFN $\gamma$  with the liposomal membrane. Differences in rotational correlation time between free and liposomal hIFN $\gamma$  were attributed to immobilization of the protein on adsorption to the liposome bilayer. Disparities were detected between the average lifetimes of liposome-adsorbed hIFN $\gamma$  and hIFN $\gamma$ -liposomes, indicating that subtle changes in the Trp-36 environment took place during preparation of the liposomes via the film hydration method compared with the adsorption of hIFN $\gamma$  to the liposome surface. The results of this study indicate that association of hIFN $\gamma$  with negatively charged liposomes results in minimal changes in the secondary and tertiary structure of the protein. We conclude that all techniques used point to a full retention or restoration of the protein conformation after desorption from the liposomes. © 2000 Wiley-Liss, Inc. and the American Pharmaceutical Association *J Pharm Sci* 89: 1605–1619, 2000

**Keywords:** circular dichroism, conformation, fluorescence, interferon gamma, liposomes, stability

## INTRODUCTION

Interferon gamma (IFN $\gamma$ ) is a cytokine with antiviral, antiproliferative and immunoregulatory

properties.<sup>1–3</sup> It has been shown to be useful as an adjuvant in vaccination against cancer<sup>4,5</sup> and a variety of viral infections, such as influenza virus,<sup>6</sup> rhinovirus,<sup>7</sup> and human immunodeficiency virus (HIV) in experimental models.<sup>8</sup> To improve its adjuvant activity, IFN $\gamma$  is encapsulated in liposomes to prevent rapid degradation and clearance after administration.<sup>4,8–10</sup> The residence

Correspondence to: W. Jiskoot (Telephone: 31-30-2537308; Fax: 31-30-2517839; E-mail: w.jiskoot@pharm.uu.nl)

*Journal of Pharmaceutical Sciences*, Vol. 89, 1605–1619 (2000)  
© 2000 Wiley-Liss, Inc. and the American Pharmaceutical Association

time of liposomal recombinant human IFN $\gamma$  (hIFN $\gamma$ ) at the site of injection in mice can be prolonged up to 7 days (i.e., a 19-fold increase compared with free hIFN $\gamma$ ) by modifying the location of the protein on the liposomal bilayer or the bilayer rigidity.<sup>9</sup> From a pharmaceutical and therapeutic point of view, it is evidently important to maintain the integrity of the protein during association with and after release from the liposomes.<sup>11</sup> The interaction between the liposomal membrane and the protein should not lead to permanent conformational changes and subsequent unwanted biological effects, such as loss of activity or enhanced toxicity. This interaction is primarily electrostatic in nature.<sup>9</sup> However, the protein can be partially embedded in the lipid bilayer, depending on the lipid composition of the bilayer and the presence of hydrophobic regions in the protein.<sup>12,13</sup> Both hydrophobic and electrostatic forces play an important role in the interaction between proteins and surfaces.<sup>14–16</sup> Furthermore, protein adsorption often leads to unfolding and (subsequent) aggregation of the protein, which is pharmaceutically unacceptable. External factors, such as the pH and ionic strength of the medium, might influence the membrane–protein interactions.<sup>17–19</sup>

IFN $\gamma$  is a molecule of 17 kD that in its bioactive form exists as a homodimer tightly associated by numerous, mostly hydrophobic interhelical interactions.<sup>20</sup> Dissociation of the dimers into monomers is an endothermic process, favored by concentrations of the protein <1  $\mu$ M (17  $\mu$ g/mL) and increasing temperature.<sup>21</sup> Dissociation of the dimer at higher concentrations requires treatment with strong denaturants, such as guanidinium hydrochloride or sodium dodecyl sulfate, or reduction of the pH to <2.<sup>22</sup> IFN $\gamma$  has an isoelectric point of  $\sim$ 10, as calculated from its amino acid content, contains no disulfide bonds, and has one tryptophan residue at position 36.<sup>23</sup> The X-ray crystal structures of recombinant human and bovine IFN $\gamma$  show that they are  $\alpha$ -helical proteins containing six helices and no  $\beta$ -sheet structure.<sup>20,24</sup>

At a pH <7, hIFN $\gamma$  associates efficiently (>80%) with negatively charged liposomes, prepared via the film method, composed of dipalmitoyl phosphatidylcholine (DPPC), dipalmitoyl phosphatidylglycerol (DPPG), and cholesterol (CH). In contrast, interaction with neutral or positively charged liposomal membranes is much lower (5–20%).<sup>9</sup>

In this paper, we study the conformational stability of hIFN $\gamma$  interacting with and after desorption from liposomal bilayers. We use hIFN $\gamma$  association with and dissociation from empty liposomes as a model for hIFN $\gamma$ -containing liposomes prepared via the film hydration method. Circular dichroism (CD) was used to study changes in the secondary and tertiary protein structure. Steady-state and time-resolved fluorescence studies were conducted to probe the local environment and the mobility of Trp-36 before, during, and after interaction of hIFN $\gamma$  with the liposomal membrane.

## MATERIALS AND METHODS

### Materials

Dipalmitoyl phosphatidylcholine (DPPC) and dipalmitoyl phosphatidylglycerol (DPPG) were donated by Lipoid GmbH (Ludwigshafen, Germany). Recombinant human IFN $\gamma$  (specific activity  $3 \times 10^7$  U/mg, purity >99%) was kindly provided by Dr. A. Zoepfel of Boehringer Ingelheim Austria GmbH (Vienna, Austria). Cholesterol (CH), trypsin, *N*-acetyl-L-tryptophanamide (NATA), and acrylamide were obtained from Sigma (St. Louis, MO). All other reagents were of analytical grade.

### Preparation of hIFN $\gamma$ -Liposomes

Two liposome formulations were prepared by the classical film hydration method,<sup>25,26</sup> as described previously.<sup>27</sup> Briefly, a film was obtained by rotary evaporation of a solution of DPPC, DPPG, and CH in methanol at a molar ratio of 10:1:10. The lipid film was flushed with nitrogen for at least 30 min. For the first formulation, henceforth referred to as hIFN $\gamma$ -liposomes, the lipid film was subsequently hydrated at 45 °C above the individual transition temperature ( $T_m$ ) of the lipids (>41 °C for DPPC) with a sterile solution of hIFN $\gamma$  (100  $\mu$ g/mL) in 10 mM sodium-succinate-buffered 5% glucose (w/v), pH 5.0 (SBG). The resulting liposome dispersion (40 mM phospholipid) was extruded sequentially through 0.6, 0.2, 0.1, and tow-stacked 0.05 and 0.1  $\mu$ m polycarbonate membrane filters (Poretics Corporation, Livermore, CA) under nitrogen pressure. Nonliposomal hIFN $\gamma$  was removed via ultracentrifugation after addition of at least one volume of 10 mM sodium-succinate-buffered 10% sucrose (w/v), pH 5.0 (SBS), based on the difference in density between SBS- and SBG-containing liposomes to separate

the liposomes from the buffer with free hIFN $\gamma$ . After two ultracentrifugation steps, the floating liposome pellet was resuspended in SBG and analyzed within 8 days of storage at 4 °C. Empty liposomes were prepared by hydrating the lipid film with sterile SBG only and were subjected to the extrusion procedure already described.

For the second formulation, henceforth referred to as liposome-adsorbed hIFN $\gamma$ , liposomes containing solely hIFN $\gamma$  adsorbed to their outer membrane surface were prepared by incubating non-sized, empty liposomes in SBG medium containing hIFN $\gamma$  (100  $\mu$ g/mL hIFN $\gamma$  per 40 mM phospholipid). The non-adsorbed hIFN $\gamma$  was removed via ultracentrifugation in SBS medium, as already described.

### Characterization of hIFN $\gamma$ -Liposomes

IFN $\gamma$  contents of the liposomes were determined by isocratic reversed-phase high-performance liquid chromatography (HPLC). Lipids, which interfere with the HPLC analysis of hIFN $\gamma$ , were eliminated according to the extraction method of Bligh and Dyer.<sup>28</sup> The HPLC system (a Spectroflow 400 solvent delivery system from Applied Biosystems, Milford, MA) and a Basic<sup>+</sup> Marathon autosampler (Separations, Emmen, The Netherlands) was equipped with a 250  $\times$  4.6 mm MacroSphere reversed-phase C18 column with a pore size of 300 Å and a particle size of 5  $\mu$ m. The column was protected with a 1-cm reversed-phase (C18) guard column (Alltech, Laarne, Belgium) and was kept at 40 °C in a water bath. The mobile phase was composed of 44% (w/w) acetonitrile in water supplemented with 10 mM sodium perchlorate and 100 mM perchloric acid. The flow was maintained at 1.00 mL/min. A 783A ultraviolet (UV) detector at 205 nm (Applied Biosystems, Milford, MA) was used for detection. Phospholipid concentrations were determined according to the method of Rouser.<sup>29</sup>

The particle size of the liposome preparations was determined by dynamic light scattering (DLS) at 25 °C with a Malvern 4700 system using a 75 mW Argon ion laser (488 nm, Uniphase, San José, CA) equipped with a remote interface controller and the PCS software, version 1.35 (Malvern Ltd., Malvern, UK). The particle size is expressed as Z-averaged diameter and the size distribution as polydispersity index (PD), ranging from 0.0 for an entirely monodisperse dispersion up to 1.0 for a polydisperse dispersion. Zeta potential measurements were performed in a Mal-

vern Zetasizer 2000, using an aqueous dip-in cell (Malvern Ltd., Malvern, UK) and PCS software, version 1.35 (Malvern Ltd., Malvern, UK) in SBG at 25 °C. Adjustment was made for the viscosity of the medium for calculation of both particle size and zeta potential. Instrument readings were checked by using latex beads with a known size and zeta potential, respectively.

### Quantification of hIFN $\gamma$ Located on the External Surface of the Liposomes

To determine the fraction of liposome-bound hIFN $\gamma$  exposed to the external dispersion medium, liposomes were incubated with medium containing the proteolytic enzyme trypsin. To the liposomal hIFN $\gamma$  dispersion (hIFN $\gamma$  concentration 100  $\mu$ g/mL), trypsin in phosphate buffered saline (PBS, pH 7.4) was added to a final concentration of 20  $\mu$ g/mL. After a 1-h incubation at 37 °C, samples were subjected to the lipid extraction procedure of Bligh and Dyer<sup>28</sup> to remove the phospholipids. The amount of remaining encapsulated hIFN $\gamma$  protected from enzymatic digestion was determined by HPLC.

### Dissociation of Surface-Bound hIFN $\gamma$ from Liposomes

To dissociate hIFN $\gamma$  from the external liposome membrane, the liposome dispersion (4.5 mL in SBS) was incubated in succinate-buffered medium containing 1.8% NaCl instead of sugar (4.5 mL SBN) for 30 min at room temperature.<sup>9</sup> Due to electrostatic shielding of the negatively charged membrane, the positively charged protein is desorbed (>85%) from the liposome surface. The hIFN $\gamma$ -containing medium was collected after ultracentrifugation and used for further study.

### Circular Dichroism Measurements

Circular dichroism (CD) spectra were recorded at ambient temperature with a dual-beam DSM 1000 CD spectrophotometer (On-Line Instrument Systems, Bogart, GA). The subtractive double-grating monochromator was equipped with a fixed disk and holographic gratings. For far-UV measurements, gratings with 2400 lines/mm (blaze wavelength 230 nm) and 1.24-mm slits were used. For near-UV measurements, gratings with 600 lines/mm (blaze wavelength 300 nm) and 0.60-mm slits were installed. Far- and near-UV spectra were recorded from 260 to 200 nm

(path length, 0.50 mm) and from 320 to 250 nm (path length, 1.00 cm), respectively. The hIFN $\gamma$  concentration was 100  $\mu\text{g}/\text{mL}$ . Two controls of free hIFN $\gamma$  were used, one preparation of hIFN $\gamma$  in SBS and the other one in a 1:1 mixture of SBS and SBN (SBS/SBN). hIFN $\gamma$  in SBS is considered the standard, native hIFN $\gamma$  control, and the SBS/SBN system containing 0.9% NaCl is a control for the desorbed hIFN $\gamma$  that is present in this buffer after desorption. Each measurement was the average of at least five repeated scans (step resolution 1 nm, 1 s each step) from which the corresponding buffer spectrum was subtracted. The measured CD signals were converted to molar ellipticity  $[\theta]$ , based on a mean amino acid residue weight of 117.

### Steady-State Fluorescence Measurements

Steady-state fluorescence measurements were performed with a LS-50B Luminescence spectrophotometer (Perkin Elmer, Norwalk, CT). In all studies, excitation and emission bandwidths were set at 2.5 nm.

Fluorescence emission spectra on excitation at 295 nm were recorded from 300 to 450 nm of 100  $\mu\text{g}/\text{mL}$  hIFN $\gamma$  in SBS or SBN with or without addition of 20-mM empty liposomes (DPPC:DPP-G:CH, 10:1:10; 100 nm). Spectra were corrected for dilution and background.

Quenching of tryptophan fluorescence by acrylamide in the range 0–0.53 M was performed by adding aliquots of acrylamide (1.4 M in the corresponding buffer) to hIFN $\gamma$  (100  $\mu\text{g}/\text{mL}$ ). To avoid interference by acrylamide absorption, the excitation wavelength used was 300 nm. The fluorescence intensity was monitored at 345 nm. The data were analyzed by a modified form of the Stern–Volmer equation:  $F_0/F = 1 + K_{\text{SV}} \cdot [\text{Q}] \cdot e^{V[\text{Q}]}$ , where  $F_0$  and  $F$  are the fluorescence intensities in the absence and presence, respectively, of the quencher (acrylamide) at concentration  $[\text{Q}]$ ,  $K_{\text{SV}}$  is the Stern–Volmer constant for dynamic quenching, and  $V$  is a constant representing static contributions to the quenching.<sup>30</sup>

### Time-Resolved Fluorescence Measurements

Time-resolved fluorescence measurements were carried out on a time-correlated single photon counting instrument equipped with mode-locked continuous wave lasers, as described elsewhere.<sup>31–35</sup> Briefly, a mode-locked CW Yttrium Lithium Fluoride (YLF) laser [Coherent model

Antares 76-YLF, Coherent Inc., Santa Clara, CA<sup>31</sup>], which was equipped with an LBO frequency doubler to obtain output at 527 nm wavelength, was used for the synchronous pumping of a cavity-dumped Rhodamine 6G dye laser (Coherent model 701-2 CD). The wavelength of the light output of the dye laser was tuned to 600 nm, and then frequency was doubled using a BBO crystal (Gsänger,  $3 \times 4 \times 7 \text{ mm}^3$ ). Emission was measured through an interference filter (Schott 343.2 or 348.8 nm). The repetition rate of excitation pulses of 300 nm was 951 kHz, the duration about 4 ps full width at half maximum (FWHM), and the excitation light was vertically polarized.

The samples were put in 12- $\mu\text{L}$  and 1.5-mm lightpath fused silica cuvettes (Starna model 26.12-F/Q/1.5/Z8.5), placed in a sample holder; temperature was controlled (20 °C), by applying thermoelectric (Peltier) elements and a controller (Marlow Industries model SE 5020). By using such a small sample volume, the effects of the scattering behavior of the sample were minimized. The sample holder was placed in a housing also containing the main detection optics. Extreme care was taken to avoid artifacts from depolarization effects. At the front of the sample housing, a Glan-laser polarizer was mounted, optimizing the already vertical polarization of the input light beam. The fluorescence was collected at an angle of 90° with respect to the direction of the exciting light beam.

By reducing the energy of the excitation pulses with neutral density filters, the frequency of fluorescence photons was decreased to 30 kHz ( $\approx 3\%$  of 951 kHz<sup>33</sup>), to prevent pile-up distortion. Also other instrumental sources for distortion of data were minimized<sup>34</sup> to below the noise level of normal photon statistics. Measurements consisted of repeated sequences of measuring during 10-s parallel and 10-s perpendicular polarized emission. The number of sequences was chosen to yield a peak content in the data files of up to  $10^5$  counts. After measuring the fluorescence of the sample, the background emission of the buffer solution was measured and used for background subtraction. All cuvettes were cleaned and checked for background luminescence prior to the measurements. The applied solvents were all fluorescence spectroscopy grade or Nanopure™ water, and tested for artificial luminescence. For obtaining a dynamic instrumental response of the experimental setup, the fast and single exponential fluorescence decay was measured of para-terphenyl in a solution of a 50/50% cyclohexane and  $\text{CCl}_4$  mix-

ture. Data analysis was performed using a home-built computer program.<sup>35,36</sup>

## RESULTS

### Characterization of hIFN $\gamma$ -Liposomes

hIFN $\gamma$  associated efficiently with solid-state DPPC:DPPG:CH (10:1:10) liposomes, prepared via the film hydration method under the chosen conditions (pH 5, low ionic strength). In a protein:lipid ratio of 1:300 (w/w), the association efficiency was  $80 \pm 7\%$  (mean  $\pm$  SD,  $n = 4$ ). From this hIFN $\gamma$  fraction,  $31 \pm 3\%$  was located at the external surface of the liposomes, as was determined with the trypsin assay.

To minimize the interference of liposomes during CD and fluorescence measurements, the liposomes were sized. After extrusion through polycarbonate filters, the zeta potential was  $-36 \pm 6$  mV and the liposome size was  $105 \pm 3$  nm (PD 0.12).

### Characterization of Adsorption of hIFN $\gamma$ to Empty Liposomes

When empty, preformed liposomes of  $69 \pm 1$  nm (PD 0.08) were incubated with a solution of free

hIFN $\gamma$  ( $50\text{--}100$   $\mu\text{g}$  per  $20$   $\mu\text{mol}$  phospholipid),  $85 \pm 9\%$  of the added hIFN $\gamma$  associated with the liposomal membranes. After incubation in  $0.9\%$  NaCl and separation of the liposomes from the medium via ultracentrifugation,  $91 \pm 3\%$  of the adsorbed hIFN $\gamma$  was desorbed. As soon as hIFN $\gamma$  was added to sized, empty liposomes, aggregation of the liposomes occurred at protein:lipid ratios  $>6$   $\mu\text{g}/\mu\text{mol}$  phospholipid, independent of the order of addition. Thus, a relatively low ratio ( $5$   $\mu\text{g}$  hIFN $\gamma/\mu\text{mol}$  phospholipid), which did not lead to measurable liposome aggregation, must be chosen to perform CD and fluorescence measurements.

### Circular Dichroism Measurements

To study the secondary and tertiary structure of hIFN $\gamma$ , far- and near-UV CD measurements were performed, respectively. The measurements were performed down to  $200$  nm, because of a too high solvent absorbance at lower wavelengths. As shown in Figure 1, free hIFN $\gamma$ , in both buffer systems, exhibits strong negative bands in the far-UV spectrum, with minima at  $208$  and  $222$  nm. The corresponding intensities with an approximate molar ellipticity of  $-2.3 \times 10^4$  and  $-2.1 \times 10^4$

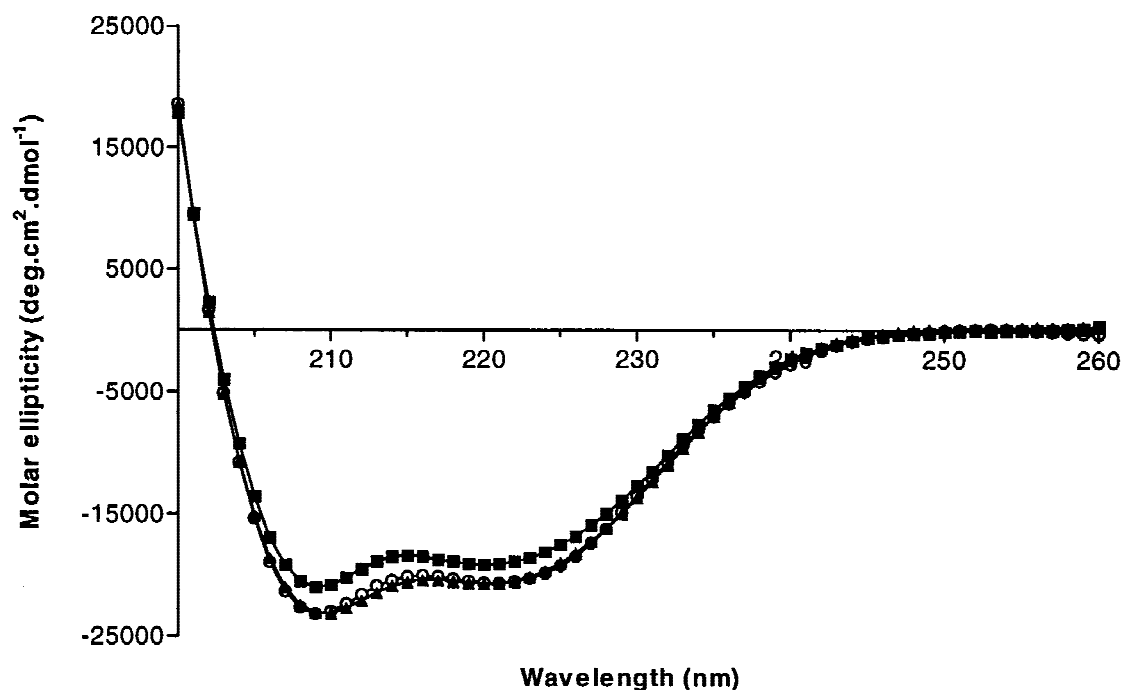


**Figure 1.** Far-UV CD spectra of hIFN $\gamma$  before association and after desorption from DPPC:DPPG:CH (10:1:10) liposomes. Key: (○) hIFN $\gamma$  in SBS; (■) hIFN $\gamma$  in SBS/SBN (1:1 (v/v)); (▲) hIFN $\gamma$  desorbed from empty DPPC:DPPG:CH (10:1:10) liposomes.

deg · cm<sup>2</sup> · dmol<sup>-1</sup>, respectively, are indicative of the predominant presence of  $\alpha$ -helical structures. hIFN $\gamma$  desorbed from empty liposomes shows a similar far-UV spectrum (Figure 1). This result means that the  $\alpha$ -helical content of hIFN $\gamma$  after adsorption to and desorption from empty liposomes is not substantially different from that of native hIFN $\gamma$ . If any change in secondary structure had occurred in the adsorbed state, this change would be fully reversible.

To investigate whether liposome-associated hIFN $\gamma$  has an altered secondary structure, far-UV CD was also performed for hIFN $\gamma$ -liposomes and liposome-adsorbed hIFN $\gamma$ . Below 220 nm, a large background signal of liposomes prevented accurate measurements. As shown in Figure 2, no major differences in spectra from 220 to 260 nm were observed, which strongly indicates that encapsulation in or adsorption to liposomes of hIFN $\gamma$  does not induce substantial changes in the secondary structure of hIFN $\gamma$ .

The near-UV spectrum of free hIFN $\gamma$  (Figure 3) shows a positive band at ~280 nm, with an approximate molar ellipticity of 140 deg · cm<sup>2</sup> · dmol<sup>-1</sup>.<sup>19,37</sup> The near-UV spectra illustrate that the tertiary structure of hIFN $\gamma$  desorbed from empty liposomes is not affected. The small differences in intensity (not in spectral shape) might be

caused by differences in protein concentration, as determined by HPLC. A too high turbidity of liposomal hIFN $\gamma$  samples did not permit near-UV CD measurements of liposome-associated hIFN $\gamma$ .

### Steady-State Fluorescence Measurements

To monitor possible changes in the direct environment of the sole tryptophan residue, fluorescence emission spectra were recorded. An emission maximum ( $\lambda_{\text{max}}$ ) was observed at 341 nm for free hIFN $\gamma$  and liposomal hIFN $\gamma$  preparations, as well as for hIFN $\gamma$  that was desorbed from empty liposomes (Figure 4). Also, the fluorescence intensity of desorbed hIFN $\gamma$  was the same as that of untreated hIFN $\gamma$ . It was not possible to accurately determine the fluorescence intensity of liposome-associated hIFN $\gamma$  because of a high background signal.

To examine the accessibility of the Trp-36 residue in hIFN $\gamma$ , acrylamide was used as a non-charged quencher. *N*-Acetyl-tryptophanamide (NATA) was used as a reference compound that is fully and easily accessible to the quencher and that is characterized by a high  $K_{\text{sv}}$  value (Figure 5 and Table 1). Trp-36 in free hIFN $\gamma$  in SBS or SBS/SBN was completely accessible to the quencher,

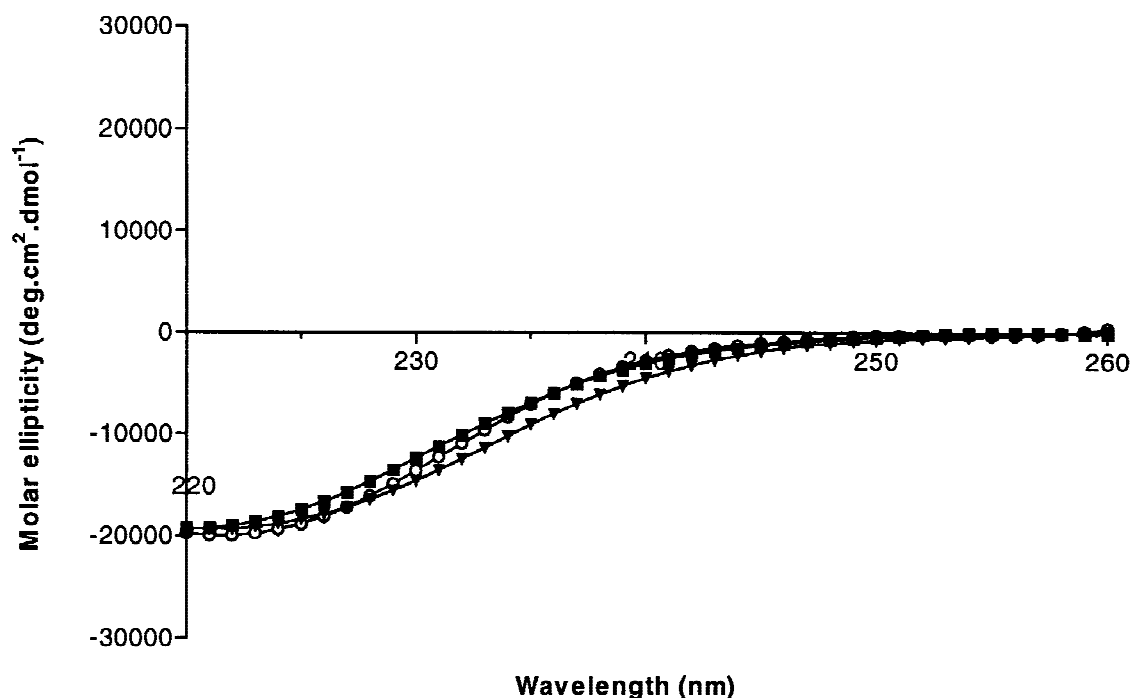


**Figure 2.** Far-UV CD spectra of hIFN $\gamma$  in SBS (○), hIFN $\gamma$ -liposomes (■), and hIFN $\gamma$  adsorbed to empty DPPC:DPPG:CH (10:1:10) liposomes (▲).

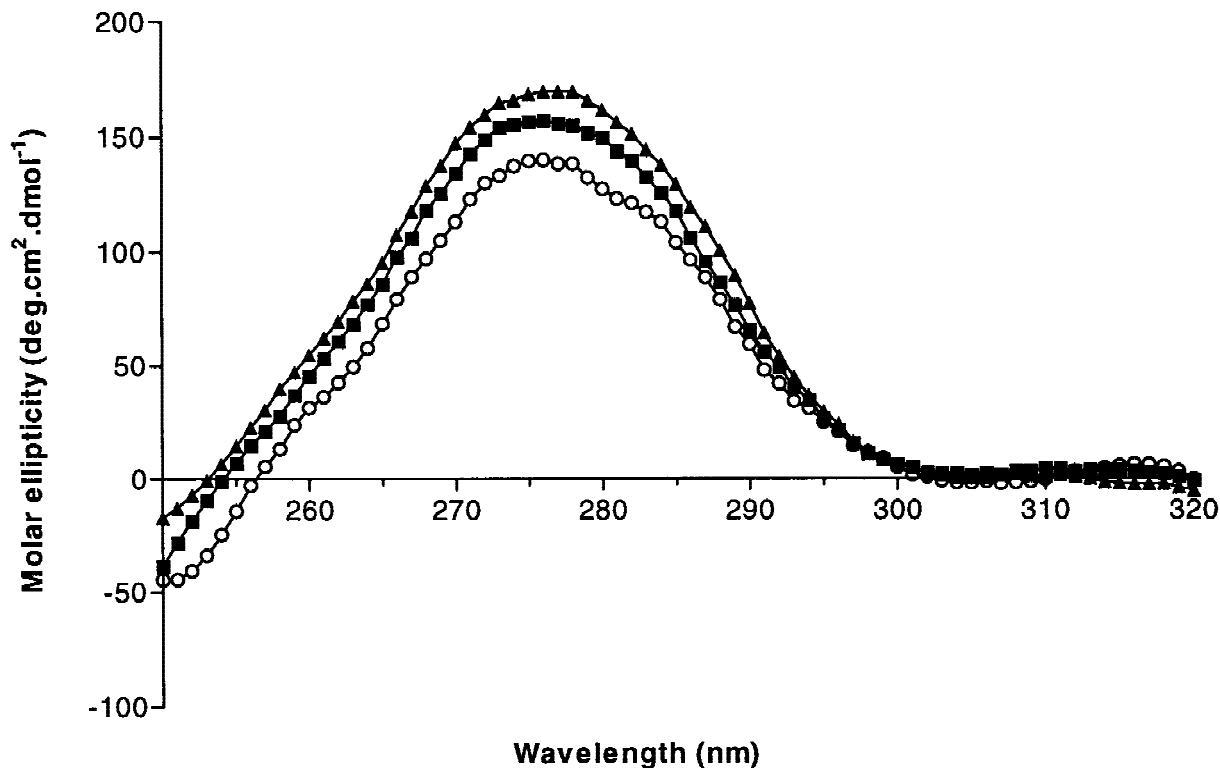


**Figure 3.** Near-UV CD spectra of hIFN $\gamma$  before association and after desorption from DPPC:DPPG:CH (10:1:10) liposomes. Key: (○) hIFN $\gamma$  in SBS; (■) hIFN $\gamma$  in SBS/SBN (1:1 (v/v)); (▲) hIFN $\gamma$  desorbed from empty DPPC:DPPG:CH (10:1:10) liposomes.

but not as unhindered as the Trp residue in NATA. The Stern–Volmer plots of quenched hIFN $\gamma$ , before and after desorption from DPPC:DPPG:CH (10:1:10) liposomes, are nearly identical, with comparable  $K_{sv}$  constants ( $3.69 \pm 0.16$ ,  $4.14 \pm 0.09$ , and  $3.31 \pm 0.09$  M $^{-1}$  for hIFN $\gamma$  in SBS, SBS/SBN, and liposome-desorbed hIFN $\gamma$ , respectively; Table 1). When the  $K_{sv}$  values were fixed to  $3.69$  M $^{-1}$  and the data were fitted again, the  $r^2$  values of the fits did not change substantially and the  $V$  value for desorbed hIFN $\gamma$  ( $0.43 \pm 0.02$  M $^{-1}$ ) lay between those for hIFN $\gamma$  in SBS and SBS/SBN ( $0.26 \pm 0.03$  and  $0.63 \pm 0.02$  M $^{-1}$ , respectively), indicating the similarity of the  $K_{sv}$  and  $V$  values.

#### Time-Resolved Fluorescence Measurements

A typical fluorescence decay of hIFN $\gamma$  is shown in Figure 6. The results of the fluorescence lifetime analysis are summarized in Table 2. Two lifetimes were observed for hIFN $\gamma$ . This result is in accord with previous studies.<sup>21,38</sup> The individual lifetime values of liposome-desorbed hIFN $\gamma$  were

slightly increased and the contribution of the short lifetime was increased ( $p_1 = 41.1\%$ ), as compared with untreated hIFN $\gamma$  in SBS or SBS/SBN buffer ( $p_1 = 15.8$ – $16.2\%$ ). However, the confidence intervals of both the pre-exponential factors and the lifetimes overlapped with those of untreated hIFN $\gamma$ , and the average lifetimes of all free hIFN $\gamma$  formulations were comparable (Table 2). To confirm the similarity of the fluorescence decays of desorbed and untreated hIFN $\gamma$ , the data of these samples were fitted by global analysis with one of the lifetimes ( $\tau_1$ ) linked across the data sets. The results (Table 3) show that both the second lifetime component ( $\tau_2$ ) and the preexponentials ( $p_1$  and  $p_2$ ) converged across the data sets. This convergence, together with the fact that the overall  $X^2$  hardly increased when linking  $\tau_1$  ( $X^2 = 1.37$  instead of  $1.33$  for unlinked data sets), led us to the conclusion that the fluorescence decays of untreated and desorbed hIFN $\gamma$  are indistinguishable.

When adsorbed to empty liposomes, hIFN $\gamma$  showed nearly the same lifetimes and relative

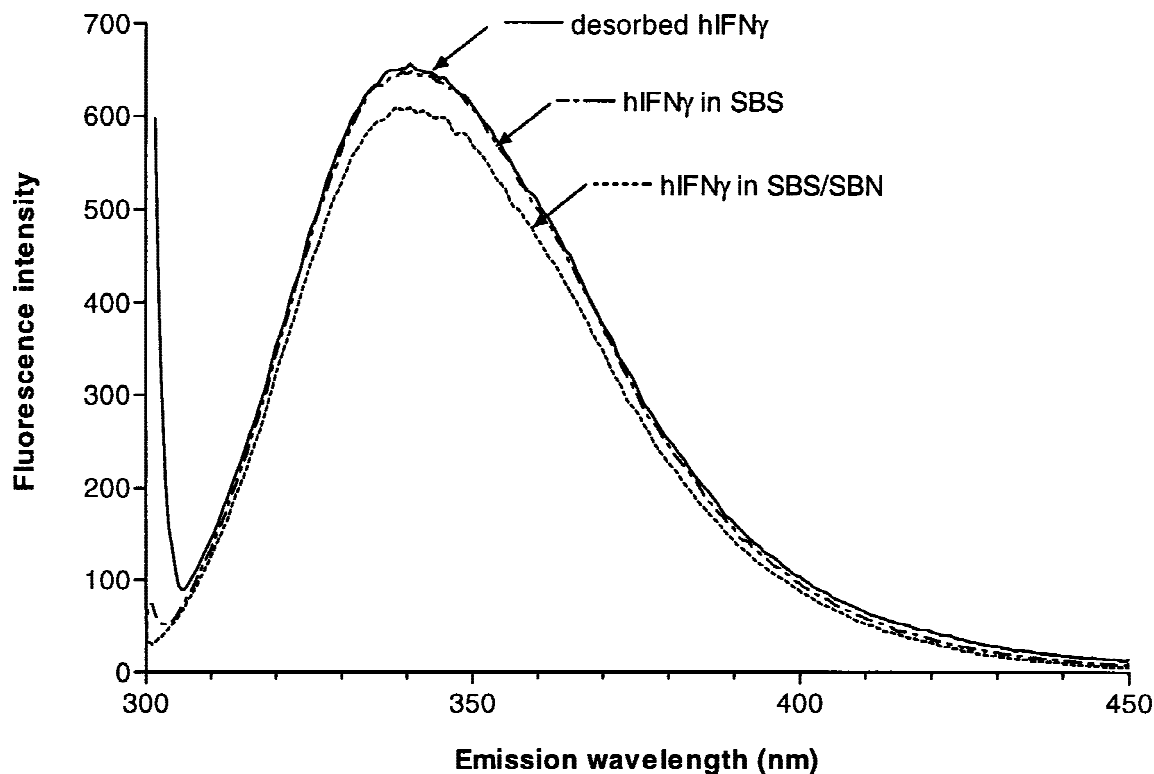


**Figure 4.** Fluorescence emission spectrum of hIFN $\gamma$  formulations, excited at 295 nm. Key: (dot/striped line) hIFN $\gamma$  in SBS; (dotted line) hIFN $\gamma$  in SBS/SBN (1:1 (v/v)); (solid line) hIFN $\gamma$  desorbed from empty DPPC:DPPG:CH (10:1:10) liposomes.

contributions as did untreated hIFN $\gamma$ . When hIFN $\gamma$  was associated with the liposomes via the film hydration method, the average lifetime decreased (2.03 ns), and a third, subnanosecond lifetime was needed to obtain a good fit ( $\tau_3 = 0.15$  ns,  $p_3 = 37.6\%$ ).

Polarized time-resolved fluorescence is a technique to monitor angular displacements of emission transition moments of fluorescent molecules. It has been applied to protein systems to investigate, among other factors, rapid angular fluctuations and protein hydrodynamics. A typical fluorescence anisotropy decay curve of hIFN $\gamma$  in SBS is shown in Figure 7. Rotational correlation times ( $\phi$ ) were determined from polarized time-resolved fluorescence intensity measurements. In all cases, only one rotational correlation time could be detected. The values for free hIFN $\gamma$  ( $\phi = 23.8$ – $27.6$  ns, Table 4), are likely to represent global motion of hIFN $\gamma$  dimers. There was no evidence of a short correlation time related to local Trp-motion. On interaction with liposomes, the rotational correlation time dramatically increased to  $>100$  ns. This result suggests virtual immobiliza-

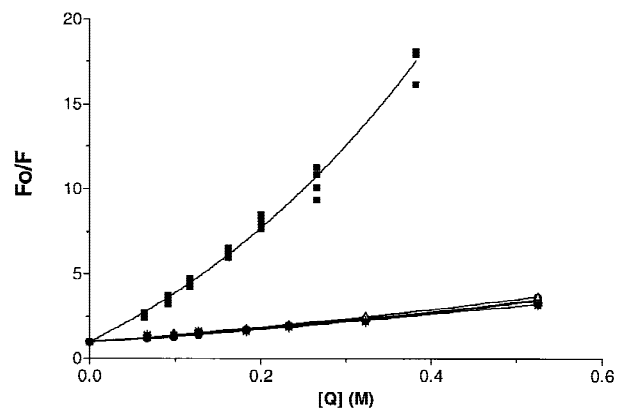


**Figure 5.** Stern–Volmer plots of the quenching of NATA and hIFN $\gamma$  fluorescence by acrylamide, before and after desorption from DPPC:DPPG:CH (10:1:10) liposomes. Quenching experiments were performed by adding aliquots of acrylamide to hIFN $\gamma$  ( $\sim 100$   $\mu\text{g/mL}$ ). NATA was diluted in SBS to yield a fluorescence signal comparable to that of hIFN $\gamma$ . The data were fitted by nonlinear regression of 4 sets of measurements using a modification of the Stern–Volmer equation:  $F_0/F = 1 + K_{sv} \cdot [Q] \cdot e^{V \cdot [Q]}$ . See Materials and Methods for more details. Key: (■) NATA; ( $\Delta$ ) hIFN $\gamma$  in SBS/SBN (1:1 (v/v)); (●) desorbed hIFN $\gamma$ ; (\*) hIFN $\gamma$  in SBS.

**Table 1.** Summary of Fluorescence Quenching Studies with Acrylamide<sup>a</sup>

Formulation	$K_{SV}$ ( $M^{-1}$ )	$V$ ( $M^{-1}$ )	$r^2$
hIFN $\gamma$ in SBS	$3.69 \pm 0.16$	$0.26 \pm 0.10$	0.9896
hIFN $\gamma$ in SBS/SBN	$4.14 \pm 0.09$	$0.38 \pm 0.05$	0.9965
Desorbed hIFN $\gamma$ <sup>b</sup>	$3.31 \pm 0.09$	$0.67 \pm 0.06$	0.9953
NATA <sup>c</sup>	$25.25 \pm 1.10$	$1.42 \pm 0.13$	0.9899

<sup>a</sup> Data were fitted according to  $F_0/F = 1 + K_{SV}[Q] \cdot e^{V[Q]}$ . The tryptophan residue was excited at 300 nm, and the intensity was read at an emission wavelength of 345 nm. See Materials and Methods for further details.

<sup>b</sup> hIFN $\gamma$  was initially adsorbed to empty DPPC:DPPG:CH (10:1:10) liposomes, and desorbed via incubation in SBS/SBN; the desorbed protein was removed via ultracentrifugation as described in Materials and Methods.

<sup>c</sup> *N*-Acetyl-L-tryptophanamide.

tion of the protein at this time scale. After desorption from the liposomes, the rotational correlation time (25.2 ns) was restored, indicating that hIFN $\gamma$  is released in its native, dimeric form (Table 4).

The presence of only one rotational correlation time implies that its fractional contribution ( $\beta$ ) equals the limiting anisotropy ( $r_0$ ). The apparent limiting fluorescence anisotropy ( $\beta$ ) was strongly reduced for both hIFN $\gamma$ -liposomes and liposomes-adsorbed hIFN $\gamma$ , compared with free hIFN $\gamma$  (Table 4).

## DISCUSSION

In this study, the conformational integrity of hIFN $\gamma$  was studied on interaction with liposomes. Evidently, protein integrity can be affected during liposome preparation, liposome association, and release from liposomes, and therefore should be carefully assessed. To our knowledge, no such information was available for hIFN $\gamma$ -liposomes until now.

hIFN $\gamma$  associates efficiently with the negatively charged DPPC:DPPG:CH (10:1:10) bilayers ( $85 \pm 9\%$ ) in a concentration range 50–500  $\mu\text{g/mL}$  hIFN $\gamma$  per 40 mM total lipid (pH 5, low ionic strength), whereas the association with neutral membranes composed of egg phosphatidylcholine only was low ( $8 \pm 1\%$ ). We performed the present study with the synthetic phospholipids DPPC and DPPG rather than their natural analogues purified from egg yolk used in previous studies because the latter showed considerable background fluorescence. To gain insight into the percentage

of the liposome surface covered by hIFN $\gamma$  on adsorption, a calculation was made with the following assumptions: (a) the liposome diameter is 100 nm, (b) the liposomes are unilamellar, (c) liposomes are composed of 20 mM DPPC:DPPG:CH (10:1:10) and 100  $\mu\text{g/mL}$  hIFN $\gamma$ , (d) the dimer has overall dimensions of  $\sim 6 \times 4 \times 3$  nm,<sup>20</sup> and (e) the surface area of the lipids was estimated to be 0.52 nm<sup>2</sup> for DPPC,<sup>39</sup> 0.48 nm<sup>2</sup> for DPPG,<sup>40</sup> and 0.30 nm<sup>2</sup> for CH (deduced from the work of Cruzeiro-Hansson et al.<sup>41</sup>). It was found that under these conditions (100  $\mu\text{g/mL}$  hIFN $\gamma$  per 20 mM phospholipid), <2% of the liposome surface is covered by hIFN $\gamma$  and each liposome contains on the average 25 protein molecules. Of the total external liposome surface,  $\sim 6\%$  is covered by negatively charged DPPG headgroups (i.e., one protein molecule per 162 DPPG molecules at the external side of the liposome bilayer). The large excess of DPPG with respect to hIFN $\gamma$  explains the fact that hIFN $\gamma$ , which is positively charged at pH 5, readily associates with the bilayer via electrostatic interactions, without measurably affecting the negative zeta potential of the liposomes. In addition, the low coverage of the total liposome surface by hIFN $\gamma$  is not expected to have a major influence on the bilayer structure.

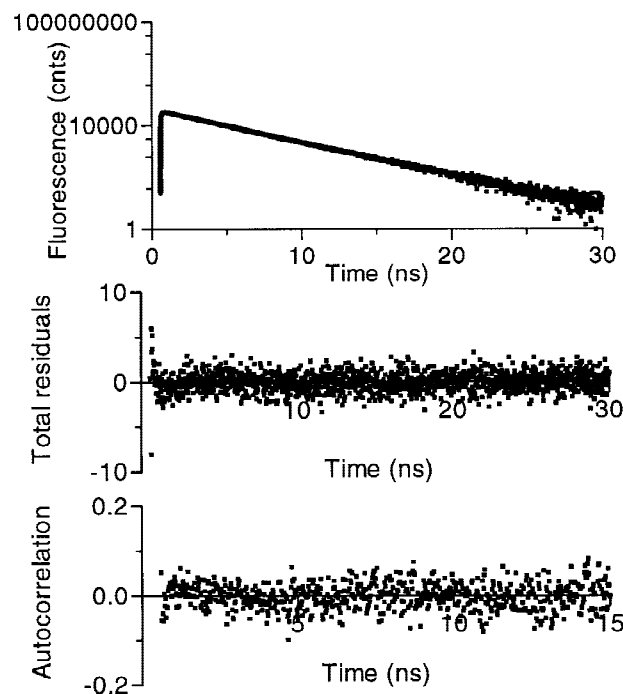


**Figure 6.** Experimental and fitted fluorescence decay of free hIFN $\gamma$  in SBS: (a) fluorescence decay, (b) fluorescence residuals, and (c) fluorescence autocorrelation.

**Table 2.** Fluorescence Lifetimes of Trp-36 in hIFN $\gamma^a$ 

Description	$p_1$ (%) <sup>b</sup>	$p_2$ (%)	$\tau_1$ (ns)	$\tau_2$ (ns)	$\tau_{av}$ (ns)	$X^2$
hIFN $\gamma$ in SBS	15.8 (10.4–29.5)	84.2 (74.2–89.4)	1.65 (1.14–2.34)	3.47 (3.43–3.61)	3.18	1.30
hIFN $\gamma$ in SBS/SBN	16.2 (11.3–26.7)	83.8 (75.8–88.3)	1.60 (1.19–2.22)	3.44 (3.40–3.55)	3.14	1.36
Desorbed hIFN $\gamma$	41.1 (20.7–71.4)	58.9 (36.0–77.1)	2.45 (1.96–2.92)	3.82 (3.60–4.33)	3.26	1.34
hIFN $\gamma$ , adsorbed						
to liposomes	14.7 (12.5–16.2)	85.5 (ND) <sup>d</sup>	0.96 (0.73–1.19)	3.52 (ND)	3.16	1.24
hIFN $\gamma$ -liposomes <sup>c</sup>	28.3 (ND)	34.1 (ND)	2.09 (ND)	4.05 (ND)	2.03	1.21

<sup>a</sup> Values between brackets represent confidence limits at the 67% level. Reduced  $X^2$  values indicate goodness of fit.

<sup>b</sup>  $p_1$  and  $p_2$  are normalized preexponential factors belonging to lifetimes  $\tau_1$  and  $\tau_2$ , respectively.

<sup>c</sup> One additional lifetime needed for good fit:  $\tau_3 = 0.15$  ns ( $p_3 = 37.6\%$ ).

<sup>d</sup> ND = not determined.

hIFN $\gamma$  is a nonglycosylated globular protein, consisting of two identical polypeptides that are tightly associated via multiple, hydrophobic inter-helical interactions. X-ray crystallography, and CD and infrared (IR) measurements revealed that the dimer has one axis of symmetry and consists of mainly  $\alpha$ -helices and no  $\beta$ -sheets.<sup>22,42</sup> Each subunit contains one tryptophan residue at position 36, which is highly conserved in all IFN $\gamma$  species sequenced until now.<sup>1,20,22,43</sup>

Unfortunately, only a low-resolution three-dimensional (3D) X-ray crystal structure of recombinant hIFN $\gamma$  is available at this moment.<sup>20</sup> Therefore, we used a 3D structure derived from bovine IFN $\gamma$  with a resolution of 2 Å to visualize the exact location of Trp-36. To illustrate the similarity between the structure of bovine and human IFN $\gamma$ , the two helical backbone structures are superimposed in Figure 8.

In Figures 8 and 9, it is clearly visible that the Trp-36 residues located at the outer side of an  $\alpha$ -helical turn are pointed inwards and embedded in the helix. Also, it is reasonable to assume that both tryptophans in the dimer are in the same environment (Figure 8), and therefore show indistinguishable fluorescence behavior.

Hoshino et al.<sup>17</sup> showed that changes in the environment of the Trp-36 residue result in a de-

creased antiviral activity, indicating the importance of this region for biological activity. It is imaginable that on interaction with a liposomal bilayer, the dimer dissociates and that hIFN $\gamma$  binds in its monomeric form to the surface, with its hydrophobic regions exposed to the hydrophobic interior of the bilayer. If so, the hIFN $\gamma$  monomers should refold to the native dimer when released from the liposome surface to regain its biological activity.

To mimic the release of hIFN $\gamma$  from liposomes, hIFN $\gamma$  was desorbed from liposomes via electrostatic shielding of the negatively charged DPPG headgroups and the positively charged hIFN $\gamma$  by NaCl. More than 90% of the adsorbed hIFN $\gamma$  was desorbed from the bilayer. To monitor possible changes in the surrounding milieu of Trp-36, steady-state fluorescence emission spectra were recorded.

The spectra correspond well with that of native hIFN $\gamma$  as reported previously.<sup>21</sup> No shift in  $\lambda_{max}$  was observed for the untreated and desorbed hIFN $\gamma$ . This result indicates that the environment of the Trp-36 residue was restored on release or retained after association with and desorption from the liposomes. The difference between the  $\lambda_{max}$  of all free hIFN $\gamma$  formulations (341 nm) and the high  $\lambda_{max}$  of NATA (356 nm), in

**Table 3.** Global Analysis of the Fluorescence Decay of Trp-36 in Untreated and Desorbed hIFN $\gamma^a$ 

Description	$p_1$ (%)	$p_2$ (%)	$\tau_1$ (ns)	$\tau_2$ (ns)	$\tau_{av}$ (ns)
hIFN $\gamma$ in SBS	19.9 (13.4–28.7)	80.1 (ND)	1.93 (1.54–2.25)	3.51 (3.41–3.60)	3.19
hIFN $\gamma$ in SBS/SBN	21.0 (14.3–30.1)	79.0 (ND)	1.93 (1.54–2.25)	3.49 (3.39–3.59)	3.16
Desorbed hIFN $\gamma$	23.6 (16.5–32.9)	76.4 (ND)	1.93 (1.54–2.25)	3.64 (3.53–3.74)	3.23

<sup>a</sup> The three data sets were fitted simultaneously with  $\tau_1$  linked across the data sets. Global  $X^2 = 1.37$  (cf. global  $X^2 = 1.33$  for the data sets fitted without any links). See Table 2 for further explanation.

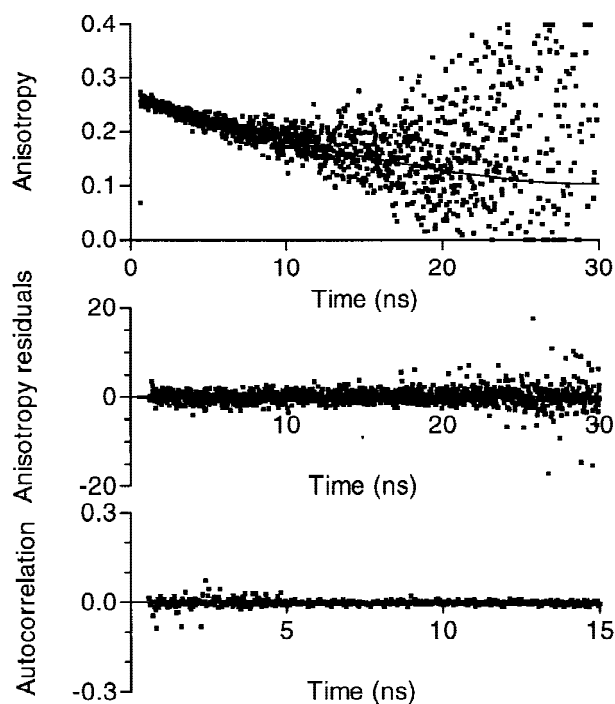


**Figure 7.** Experimental and fitted anisotropy decay curves constructed from the individual polarized decay curves of free hIFN $\gamma$  in SBS: (a) fluorescence anisotropy decay, (b) fluorescence anisotropy residuals, and (c) fluorescence anisotropy autocorrelation.

which the Trp-residue is in direct contact with the aqueous solvent, indicates that Trp-36 is not completely exposed to the aqueous buffer but surrounded by less hydrophilic moieties of the polypeptide backbone. This suggestion is supported by the elucidated X-ray crystal structure. Figure 9 shows that the C $\alpha$  atom of Trp-36 is located at the outside of the protein, but the indole side chain is faced towards the protein interior.

In the fluorescence quenching studies, acrylamide, a small neutral molecule ( $M_w$  71), was used as a quencher that is able to penetrate into

the hydrophobic pockets of the protein. The upward curvature in the Stern–Volmer plot (Figure 5) indicates full accessibility of the Trp-residue for the quencher, although both the dynamic and static components,  $K_{sv}$  and  $V$ , were much lower than for NATA (see Table 1). The relatively small values of the quenching constants support the conclusion drawn from the fluorescence emission spectrum; that is, Trp-36 is not fully exposed to the aqueous solvent.

The far- and near-UV spectra of desorbed hIFN $\gamma$  are similar to the spectra of untreated hIFN $\gamma$  and correspond to the spectra of native hIFN $\gamma$  as reported in the literature,<sup>42</sup> indicating the preservation of the secondary and tertiary structure after desorption. The far-UV CD spectra of hIFN $\gamma$ –liposomes and liposome-adsorbed hIFN $\gamma$  also show only marginal differences with the untreated hIFN $\gamma$  in SBS. Although it was not possible to analyze the spectra below 220 nm, the data suggest that no large changes in secondary structure of hIFN $\gamma$  occur during either mode of interaction with liposomes.

Although the steady-state fluorescence technique is very sensitive to structural changes in the vicinity of the fluorophore, the information obtained from these experiments cannot fully explain the molecular origin of the observed effect. Moreover, the relatively low protein-to-lipid ratio, which was mandatory to prevent aggregation of liposome-adsorbed hIFN $\gamma$  formulations, did not permit accurate intensity measurements of liposome-associated hIFN $\gamma$ . The relatively high lipid concentration, in combination with the not fully monochromatic excitation source of the steady-state fluorimeter, resulted in a large scatter signal. In contrast, because the fluorescence lifetime instrument is equipped with monochromatic laser light and a more sensitive detection system, we were able to compare the local mobility of Trp-36 and the rotational behavior of hIFN $\gamma$  before, dur-

**Table 4.** Rotational Correlation Times of Trp-36 in hIFN $\gamma^a$

Description	$\beta$	$\phi$ (ns)	$X^2$
hIFN $\gamma$ , 10% sucrose	0.257 (0.254–0.262)	27.6 (24.6–31.0)	1.39
hIFN $\gamma$ , 5% sucrose + 0.9% NaCl	0.256 (0.254–0.261)	23.8 (21.4–26.3)	1.38
Desorbed hIFN $\gamma$	0.243 (0.240–0.247)	25.2 (22.9–28.2)	1.36
hIFN $\gamma$ , adsorbed to liposomes	0.136 (0.131–0.141)	>100	1.27
hIFN $\gamma$ -liposomes	0.121 (0.117–0.124)	>100	1.26

<sup>a</sup> Values between brackets represent confidence limits at the 67% level. Reduced  $X^2$  values indicate goodness of fit.

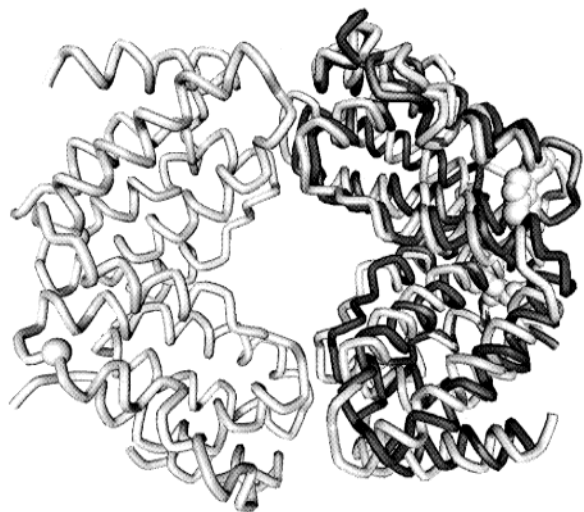


**Figure 8.** Ribbon drawing of the crystal structure of bovine IFN $\gamma$  overlaid with hIFN $\gamma$ . The dark gray ribbon represents one hIFN $\gamma$  dimer. The light gray structure represents the tetrameric form of bovine IFN $\gamma$ . Light gray spheres are the Trp residues. The structure of bovine IFN $\gamma$  was solved with X-ray crystallography to a resolution of 2.0 Å and deposited at the Protein Data Bank (RCSB) under the code 1d9c by M. Randal and A. A. Kossiakoff.<sup>24</sup>

ing, and after association with sized, empty DP-PC:DPPG:CH (10:1:10) liposomes using (polarized) time-resolved fluorescence. Because the excited state of the fluorophore has a half-life in the nanosecond range, corresponding to the time scale of many biological processes (diffusion of small molecules, rotational and internal motions, etc.), time-resolved fluorescence spectroscopy can provide information on physicochemical processes, the structure, and the dynamics of the surroundings of the fluorophore. Small protein aggregates usually not detectable with classical spectroscopic methods can be detected as well.<sup>38</sup> In our study, the average lifetimes ( $\tau_{av}$ ) of free hIFN $\gamma$  and hIFN $\gamma$  adsorbed to liposomes are equivalent and identical to previously reported values,<sup>21</sup> although slight differences in relative contribution and individual lifetimes were observed (Table 2). In contrast, for hIFN $\gamma$ -liposomes  $\tau_{av}$  was considerably reduced and a third lifetime of 0.15 ns was needed to fit the decay curve. The difference between the decay of hIFN $\gamma$ -liposomes and liposome-adsorbed hIFN $\gamma$  may indicate the occurrence of a minimal alteration in the local Trp-36 environment during the

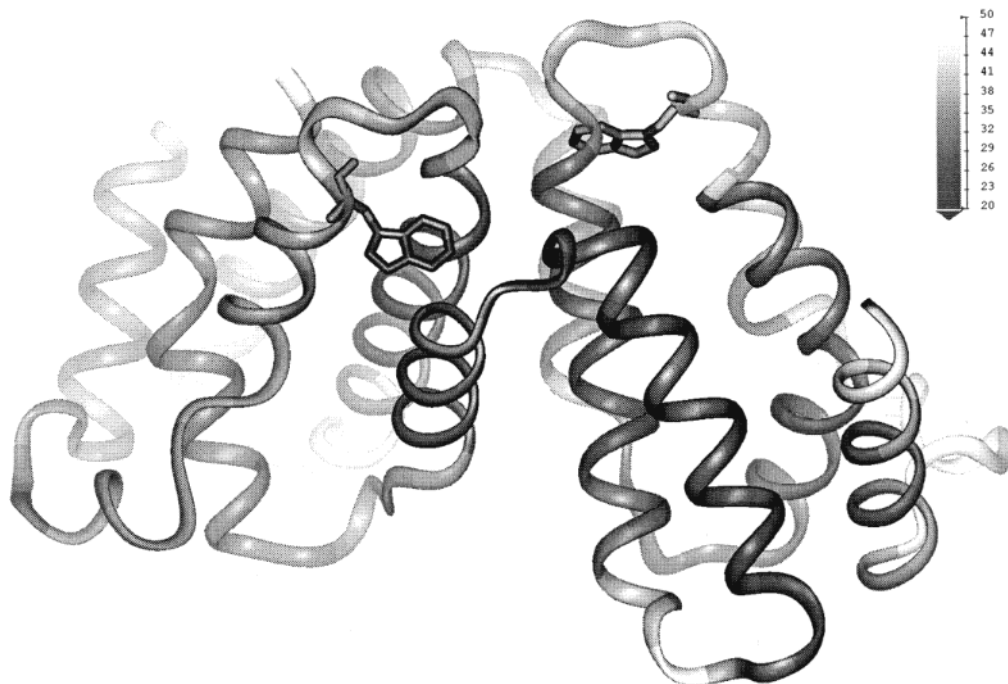


**Figure 9.** Ribbon drawing of the crystal structure of bovine IFN $\gamma$ . Shading according to the isotropic temperature factor (B-factor) visualizing the mobility of the amino acid residues (light is very mobile; dark is very inflexible). The structure of bovine IFN $\gamma$  was solved with X-ray crystallography to a resolution of 2.0 Å and deposited at the Protein Data Bank (RCSB) under the code 1d9c by M. Randal and A. A. Kossiakoff.<sup>24</sup>

film hydration process or on centrifugation and extrusion of the hIFN $\gamma$ -liposome dispersion. The fact that neither the far-UV CD spectra (Figure 2) nor the fluorescence emission maximum showed differences between free hIFN $\gamma$  and liposomal hIFN $\gamma$  indicates that such a change would be subtle indeed.

The rotational correlation times found for free hIFN $\gamma$ , both untreated and after desorption (Table 4), are in agreement with the literature values for native hIFN $\gamma$ ,<sup>21</sup> indicating that hIFN $\gamma$  is still in its native, dimeric form after release from the liposomes. The observed rotational correlation time (~25 ns) lies between those reported for lysozyme ( $\phi \approx 10$  ns,  $M_r \approx 17$  kD) and albumin ( $\phi \sim 42$  ns,  $M_r \approx 67$  kD),<sup>44</sup> and is thus in excellent agreement with a rotational correlation time expected for a hIFN $\gamma$  dimer ( $M_r \approx 34$  kD). Association with liposomes, either via adsorption or encapsulation, prolonged the rotational correlation time infinitely on this time scale, indicating that essentially all protein molecules are immobilized through association with the liposomal bilayer.

No short correlation time (<2 ns), typical for local mobility of the fluorophore, was observed. This result can be explained by rigidifying interactions between Trp-36 with the surrounding residues in the  $\alpha$ -helices. Specifically, as elucidated with LIGPLOT,<sup>45</sup> Trp-36 of one monomer (chain A) forms hydrogen bridges with Ile-32, Glu-39 from the same monomer, and Asp-91 of the other monomer (chain B). It exhibits hydrophobic contacts with Lys-42, Ile-45 from chain A, and Lys-88 from chain B. These interactions are translated in a low isotropic temperature factor (or B-factor, theoretically describing the thermal vibration of a crystal<sup>46</sup>), as visualized in Figure 9. It is noteworthy to mention that both X-ray crystallography and time-resolved fluorescence results suggest an immobile state of the Trp-36 residue. Moreover, the results of time-resolved fluorescence anisotropy, fluorescence quenching studies, and fluorescence emission spectra are complementary in that they all support the inward direction of Trp-36.

The limiting anisotropy values ( $\beta$ ) for free and desorbed hIFN $\gamma$  correspond well with earlier reported values for native hIFN $\gamma$ .<sup>21,38,47</sup> However, for both liposomal hIFN $\gamma$  preparations, a reduction in  $\beta$ -value is apparent. Because the limiting anisotropy is an intrinsic tryptophan property and, in principle, independent from any environmental factor (except for the excitation wave-

length, which was fixed), this reduction is difficult to explain. An explanation might be that an ultrafast, nonrotational depolarization occurred during the latency time of the data acquisition circuitry of the instrument (i.e., <40 ps). Energy transfer is an obvious nonrotational depolarization mode, but would only be possible if two Trp residues were almost stacked. This explanation seems unlikely when considering the position of Trp-36 (see Figure 8).

In conclusion, the results of this study indicate that association of hIFN $\gamma$  with negatively charged liposomes results in minimal changes in the secondary and tertiary structure of the protein both during association with and after desorption from the liposomal bilayer. Differences in rotational correlation time between free and liposomal hIFN $\gamma$  were attributed to an immobilization of the protein after adsorption to the liposome bilayer. Only slight differences were detected between the average lifetimes of liposome-adsorbed hIFN $\gamma$  and hIFN $\gamma$ -liposomes, indicating that subtle changes in the Trp-36 environment took place during preparation of the liposomes via the film hydration method compared with the adsorption of hIFN $\gamma$  to the liposome surface.

## ACKNOWLEDGMENTS

We are grateful to Dr. E. Moret of the Department of Medicinal Chemistry of the Faculty of Pharmacy, Utrecht University, for preparing the figures of crystal structure of bovine and human IFN $\gamma$ . The authors kindly thank Ms. C. Carrascosa and Ms. F. M. Ossendrijver of the Department of Pharmaceutics of the Faculty of Pharmacy, Utrecht University, for technical assistance in the preparation of liposomes and performing fluorescence measurements. Dr. A. Zoepfel from Boehringer Ingelheim Austria, Vienna, Austria, is gratefully acknowledged for the generous donation of hIFN $\gamma$ .

## REFERENCES

1. Gray PW, Goeddel DV. 1987. Molecular biology of interferon-gamma. In Goeddel DV, Webb DR, editors. *Molecular cloning and analysis of lymphokines*. Orlando: Academic Press. pp 151-162.
2. Joklik WK. 1990. Interferons. In: Knipe DM, Fields BN, editors. *Virology*. New York: Raven Press, pp 383-410.

3. Stewart II WE. 1981. Non-antiviral actions of interferons. In: Stewart II WE, editor. *The interferon system*, 2<sup>nd</sup> ed. Vienna: Springer Verlag, pp 223–256.
4. van Slooten ML, Storm G, Zoepfel A, Küpcü Z, Boerman OC, Crommelin DJA, Wagner E, Kircheis R. 2000. Liposomes containing interferon-gamma as adjuvant in tumor cell vaccines. *Pharm Res* 17: 42–48.
5. Koppenhagen FJ, Küpcü Z, Wallner G, Crommelin DJA, Wagner E, Storm G, Kircheis R. 1998. Sustained cytokine delivery for anticancer vaccination: Liposomes as alternative for gene-transfected cells. *Clin Cancer Res* 4:1881–1886.
6. Playfair JH, De-Souza JB. 1987. Recombinant gamma interferon is a potent adjuvant for a malaria vaccine in mice. *Clin Exp Immunol* 67:5–10.
7. Hayden FG, Gwaltney Jr JM. 1983. Intranasal interferon  $\alpha$ 2 for prevention of rhinovirus infection and illness. *J Infect Dis* 148:543–550.
8. Lachman LB, Shih LC, Rao XM, Hu X, Bucana CD, Ullrich SE, Cleland JL. 1995. Cytokine-containing liposomes as adjuvants for HIV subunit vaccines. *AIDS Res Hum Retroviruses* 11:921–932.
9. van Slooten ML, Boerman OC, Romøren K, Crommelin DJA, Storm G, unpublished results.
10. Herrmann J. 1991. Preparation and properties of gamma-interferon containing liposomes. Thesis. Ruprecht Karl University, Heidelberg, Germany.
11. van de Weert M, van 't Hof R, Hennink WE, Crommelin DJA. 1998. Stability of pharmaceutical proteins in particulate carriers. In: Frokjaer S, Christrup L, Krogsgaard-Larsen P, editors. *Peptide and protein drug delivery*. Copenhagen: Munksgaard, pp 359–375.
12. Lo YL, Rahman YE. 1995. Protein location in liposomes, a drug carrier: A prediction by differential scanning calorimetry. *J Pharm Sci* 84:805–814.
13. Papahadjopoulos D, Moscarello M, Eylar EH, Isac T. 1975. Effects of proteins on thermotropic phase transitions of phospholipid membranes. *Biochim Biophys Acta* 401:317–335.
14. Hlady V, Buijs J. 1996. Protein adsorption on solid surfaces. *Curr Opin Biotechnol* 7:72–77.
15. Pap EHW, Houbiers MC, Santema JS, van Hoek A, Visser AJWG. 1996. Quantitative fluorescence analysis of the adsorption of lysozyme to phospholipid vesicles. *Eur Biophys J* 24:223–231.
16. Norde W. 1995. Adsorption of proteins at solid-liquid interfaces. *Cells Mater* 5:97–112.
17. Hoshino T, Mikura Y, Shimidzu H, Kusumoto S, Kawai J, Toguchi H. 1987. Reduction in antiviral activity of human interferon-gamma in acidic media with reference to structural change. *Biochim Biophys Acta* 916:245–250.
18. Collins D, Cha Y. 1994. Interaction of recombinant granulocyte colony stimulating factor with lipid membranes: Enhanced stability of a water-soluble protein after membrane insertion. *Biochemistry* 33:4521–4526.
19. Arakawa T, Hsu YR, Yphantis DA. 1987. Acid unfolding and self-association of recombinant *Escherichia coli* derived human interferon gamma. *Biochemistry* 26:5428–5432.
20. Ealick SE, Cook WJ, Vijay-Kumar S, Carson M, Nagabhushan TL, Trotta PP, Bugg CE. 1991. Three-dimensional structure of recombinant human interferon-gamma. *Science* 252:698–702.
21. Boteva R, Zlateva T, Dorovska-Taran V, Visser AJW, Tsanev R, Salvato B. 1996. Dissociation equilibrium of human recombinant interferon gamma. *Biochemistry* 35:14825–14830.
22. Samudzi CT, Burton LE, Rubin JR. 1991. Crystal structure of recombinant rabbit interferon-gamma at 2.7-Å resolution. *J Biol Chem* 266:21791–21797.
23. Rinderknecht E, O'Connor BH, Rodriguez H. 1984. Natural human interferon-gamma. Complete amino acid sequence and determination of sites of glycosylation. *J Biol Chem* 259:67906797.
24. Randal M, Kossiakoff AA. 2000. Structure of bovine interferon-gamma; assessment of structural differences between species. *Acta Crystallogr Sect D* 56:14.
25. Amselem S, Gabizon A, Barenholz Y. 1993. A large-scale method for the preparation of sterile and non-pyrogenic liposomal formulations of defined size distributions for clinical use. In: Gregoriadis G, editor. *Liposome technology*, 2nd edition. Boca Raton, FL: CRC Press, pp 501–525.
26. Nässander UK, Storm G, Peeters PAM, Crommelin DJA. 1990. Liposomes. In: Chasim M, Langer R, editors. *Biodegradable polymers as drug delivery systems*. New York: Marcel Dekker Inc., pp 261–338.
27. van Slooten ML, Storm G, Zoepfel A, Küpcü Z, Boerman OC, Crommelin DJA, Wagner E, Kircheis R. 2000. Liposomes containing interferon-gamma as adjuvant in tumor cell vaccines. *Pharm Res* 17: 42–48.
28. Bligh EG, Dyer WS. 1959. A rapid method of total lipid extraction and purification. *Can J Biochem Physiol* 37:911–917.
29. Rouser G, Flusher S, Yamamoto A. 1970. Two dimensional thin layer chromatographic separation of polar lipids and determination of phospholipids by phosphorus analysis of spots. *Lipids* 5:494–496.
30. Lakowicz JR. 1983. *Principles of fluorescence spectroscopy*. New York: Plenum Press.
31. Reed E, Frangineas G. 1990. Design and performance of a high-power mode-locked Nd:YLF laser. *SPIE Proc* vol 1223: Solid State Lasers.
32. van Hoek A, Visser AJWG. 1990. Efficient method for the extraction of second harmonic light after extracavity frequency doubling. *Appl Optics* 29: 2661–2663.
33. Vos K, van Hoek A, Visser AJWG. 1987. Applica-

- tion of a reference deconvolution method to tryptophan fluorescence in proteins. A refined description of rotational dynamics. *Eur J Biochem* 165:55–63.
34. van Hoek A, Visser AJWG. 1985. Artifact and distortion sources in time correlated single photon counting. *Anal Instrument* 14:359–378.
  35. Novikov EG, van Hoek A, Visser AJWG, Hofstraat JW. 1999. Linear algorithms for stretched exponential decay analysis. *Opt Commun* 189–198.
  36. Digris AV, Skakoun VV, Novikov EG, van Hoek A, Claiborne A, Visser AJWG. 1999. Thermal stability of a flavoprotein assessed from associative analysis of polarized time-resolved fluorescence spectroscopy. *Eur Biophys J* 28:526–531.
  37. Hsu YR, Arakawa T. 1985. Structural studies on acid unfolding and refolding of recombinant human interferon-gamma. *Biochemistry* 24:7953–7963.
  38. Brochon JC, Tauc P, Merola F, Schoot BM. 1993. Analysis of a recombinant protein preparation on physical homogeneity and state of aggregation. *Anal Chem* 65:1028–1034.
  39. Cevc G, Seddon JM, Marsh D. 1986. The mechanism of regulation of membrane phase behaviour structure and interactions by lipid headgroups and electrolyte solution. *Faraday Discuss Chem Soc* 81: 179–189.
  40. Watts A, Harlos K, Marsh D. 1981. Charge-induced tilt in ordered-phase phosphatidylglycerol bilayers evidence from X-ray diffraction. *Biochim Biophys Acta* 645:91–96.
  41. Cruzeiro-Hansson L, Ipsen JH, Mouritsen OG. 1989. Intrinsic molecules in lipid membranes change the lipid-domain interfacial area: Cholesterol at domain interfaces. *Biochim Biophys Acta* 979:176.
  42. Kendrick BS, Cleland JL, Lam XM, Nguyen T, Randolph TW, Manning MC, Carpenter JF. 1998. Aggregation of recombinant human interferon gamma: kinetics and structural transitions. *J Pharm Sci* 87:1069–1076.
  43. Gray PW, Goeddel DV. 1983. Cloning and expression of murine immune interferon cDNA. *Proc Natl Acad Sci USA*. 80:5842–5846.
  44. Creighton TE. 1984. *Proteins: Structure and molecular principles*. New York: W. H. Freeman & Co.
  45. Wallace AC, Laskowski RA, Thornton JM. 1995. LIGPLOT: A program to generate schematic diagrams of protein-ligand interactions. *Protein Eng* 8:127–134.
  46. Priestle JP, Paris CG. 1994. Experimental techniques and data banks. In: Cohen NC, editor. *Guidebook on molecular modeling in drug design*. New York: Academic Press, pp 139–217.